EPSC2018

SB15 abstracts

EPSC Abstracts
Vol. 12, EPSC2018-136, 2018
European Planetary Science Congress 2018

Comparative analyses of two Jupiter family comets: dust-rich 67P/Churyumov-Gerasimenko and dust-poor 2P/Encke

Vera Rosenbush (1,2), Nikolai Kiselev (2,3), Oleksandra Ivanova (1,2,4), Olena Shubina (2), Dmitry Petrov (3), Valeriy Kleshchonok (1), and Viktor Afanasiev (5)
(1) Taras Shevchenko National University of Kyiv, Kyiv, Ukraine (vera.rosenbush@gmail.com), (2) Main Astronomical Observatory of the NAS of Ukraine, Kyiv, Ukraine, (3) Crimean Astrophysical Observatory, Nauchnij, Crimea, (4) Astronomical Institute of the SAS, Tatranská Lomnica, Slovak Republic, (5) Special Astrophysical Observatory of the RAS, Nizhnij Arkhyz, Russia

Abstract

The results of imaging photometric, polarimetric, and long-slit spectroscopic observations of comet 67P/Churyumov–Gerasimenko in 2015–2016, which was the target of the ESA's Rosetta mission, and a highly evolved comet 2P/Encke in apparitions of 2013 and 2017 are presented. Similar radial variations of polarization and color over the coma revealed in both comets, dust-poor comet Encke and dust-rich comet 67P/C-G, are discussed.

1. Introduction

Comet 67P/Churyumov–Gerasimenko (hereafter 67P/C-G) was the target of the ESA's Rosetta mission. Combining results of the ground-based observations with the Rosetta studies shed light on the properties of the dust particles as well as processes of their ejection and evolution. Comet 2P/Encke has a number of features that attract the attention of researchers. First of all, comet Encke is a highly evolved comet; an extremely low content of dust which is concentrated in the near-nucleus region of the coma, making Encke one of the gassiest comets; the presence of sunward-oriented fan which is observed near perihelion almost in all apparitions. Accordingly, our researches are aimed at a better understanding of these features and processes occurring in the coma of both comets.

2. Observations

Three sets of photometric, polarimetric, and spectral observations of comet 67P/C-G were carried out on November 8 and December 9 2015 and April 3–5, 2016. Heliocentric distance (r) of the comet was within the range from 1.62 au to 2.72 au, geocentric distances (Δ) from 1.81 au to 1.72 au, and phase angles (α) from 33.2° to 10.4°. Imaging polarimetric, photometric, and long-slit spectroscopic observations of comet Encke were performed at r=0.56 au, Δ=0.65 au, and α=109° on November 4, 2013 and at r=1.052 au, Δ=1.336 au, and α=46.8° on January 23, 2017. In all cases, observations were taken at the 6-m telescope with a multimode focal reducer SCORPIO-2 of the SAO RAS. A 2048 × 2048 CCD with a full field of view of 6.1'×6.1' and a pixel scale of 0.18 arcsec/px was used as a detector. Observations were acquired using the broad-band filters as well as the narrow-band cometary filters.

3. Results

The spatial distribution of intensity, color, and linear polarization over the coma showed the following features.

3.1 Comet 67P/C-G

The comet was a very active. Two persistent jets and long dust tail were observed during the whole observing period. The radial profiles of surface brightness, color, and polarization significantly differed for the coma, jets, and tail, and changed with increasing heliocentric distance. The dust production $Af\rho$ decreased from 162 cm at r = 1.62 au to 51 cm at r = 2.72 au. The dust color (g-r) gradually changed from 0.8^m in the innermost coma to ~0.4^m in the outer coma. In November and December, the polarization in the near-nucleus area was ~8%, dropped sharply to 2% at the distance ~5000 km, and then gradually

increased with distance from the nucleus, reaching ~8% at 40000 km. In April, at α=10.4°, the polarization varied between –0.6% in the near-nucleus area and –4% in the outer coma.

3.2 Comet Encke

The dust in the comet was concentrated to the near-nucleus area and only a negligible continuum signal was present at distances greater than 2000 km from the nucleus. The low dust production $Af\rho = 32\pm7$ in the BC filter confirmed the status of the comet as optically dust-poor one. The fan/tail structures were detected in the coma in both observational periods. The dust color (BC-RC) decreased from ~1.0^m in the innermost coma up to ~0.1^m at the distance 2500 km. The corrected for gas contamination radial profiles of polarization showed that the polarization in the near-nucleus area was almost 12%, dropped sharply to 6% at the distance ~3000 km, and then gradually increased to the outer coma, reaching 12% at 12000 km.

4. Analysis

Revealed radial variations of polarization and color in both comets, dust-poor comet Encke and dust-rich comet 67P/C-G, suggest a change in the particle properties and, hence, in the mean scattering properties of the grains on a time-of-flight timescale. To calculate the light scattering properties of individual scattering particles, the *Sh*-matrix method [1] for Gaussian particles was used. In the case of comet Encke, we considered cometary dust as a mixture of particles of three types: silicates, organic matter, and water ice. Our simulation allowed us to determine the microphysical parameters of the model particles which demonstrated a good agreement with the observed changes in color and polarization. Contrary, in the case of comet 67P/C-G, cometary dust was presented by particles of single type which decayed with distance from the nucleus. Calculations showed that physical decay of particles can also explain the spatial variations of polarization and color of dust in the comet.

5. Summary and Conclusions

The behavior of polarization and color with the distance from the nucleus of comet Encke *qualitatively* is similar to their behavior observed in comet 67P/C-G [2]. However, the *quantitative* changes in polarization and color with distance from the nucleus of both comets are differed. This may be partly due to different phase angles of comets, 46.8° and 33.2° for Encke and 67P/C-G, respectively. However, most of these differences can be explained by the difference in the properties of dust particles in these two comets. Firstly, the color of Encke's dust in the near-nucleus area of the coma is noticeably redder (reddening is ~15%) than that (8.2%) for comet 67P/C-G. The color change of the dust ("blueing") and the increase of polarization degree toward to the outer part of the coma in comet Encke occur faster than those in comet 67P/C-G. At the nucleocentric distances up to ~3000 km, a decrease in polarization with decreasing particle size is expected when the size of particles decreases from hundreds of microns to some microns. In order to understand how different physical properties of the dust particles affect the behavior of color and polarization, further numerical simulations of light scattering by cometary dust particles are required.

Acknowledgements

The authors express appreciation to the Large Telescope Program Committee of the RAS for the possibility of implementing the program of observations of comets 67P/Churyumov-Gerasimenko and 2P/Encke at the BTA. The researches by VR and OI are supported, in part, by the project 16BF023-02 of the Taras Shevchenko National University of Kyiv. OI thanks the SASPRO Programme, REA grant agreement No. 609427, and the Slovak Academy of Sciences (grant Vega 2/32/14).

References

[1] Petrov, D., Shkuratov, Yu., and Videen, G.: Light scattering by arbitrary shaped particles with rough surfaces: Sh-matrices approach. J. Quant. Spectrosc. Radiat. Transfer, Vol. 113, pp. 2406–2418, 2012.

[2] Rosenbush, V.K., Ivanova, O.V., Kiselev, N.N., Kolokolova, L.O., and Afanasiev, V.L.: Spatial variations of brightness, colour and polarization of dust in comet 67P/Churyumov–Gerasimenko. Mon. Not. R. Astron. Soc., Vol. 469, pp. 475–491, 2017.

EPSC Abstracts
Vol. 12, EPSC2018-251, 2018
European Planetary Science Congress 2018

(3200) Phaethon: asteroid or comet?

Alberto Cellino (1) and/for the INAF-OCA-Armagh-Rhozen-Kharkiv-Lowell Team
Maxime Devogèle; Philippe Bendjoya; Jean-Pierre Rivet, David Vernet, Lyu Abe, Stefano Bagnulo, Apostolos Christou, Galin Borisov, Z. Donchev, T. Bonev, Irina Belskaya, Yurij Krugly
(1) INAF - Astrophysical Observatory of Torino, Torino, Italy, (alberto.cellino@inaf.it)

Abstract

A multi-colour phase - polarization curve of asteroid (3200) Phaethon has been obtained during the December 2017 apparition by merging measurements taken at the observing station of Calern (France) and at the Rhozen observatory (Bulgaria). The measured values of linear polarization are among the highest ever observed for a Solar system body. The P_{max} parameter seems to occur at a phase angle around 130° and reaches more than 45%. Phaethon is the parent body of the Geminid meteor shower, and the real physical nature of this object (asteroid or comet?) has been a long-debated subject. Our polarimetric measurements suggest that Phaethon is an asteroid, rather than a comet, and is likely a former member of the dynamical family of (2) Pallas.

1. Introduction

(3200) Phaethon is a near-Earth asteroid belonging to the Apollo orbital subclass, and is a very interesting object due to a number of peculiar properties.

1. It has a very high orbital eccentricity (0.89), and a correspondingly small perihelion distance of only 0.14 AU.

2. It is thought to be the parent body of the Geminid meteor shower.

3. In terms of spectral reflectance properties it belongs to an unusual taxonomic class.

In particular, it was classified by [1] as a member of the rare F taxonomic class, whose members are low-albedo objects that in at least one case (the asteroid (4015) Wilson Harrington) have exhibited in the past some cometary activity. The F class in no longer present in the most recent classifications, because it was characterized by its behaviour at blue wavelengths, that are no longer covered in modern spectroscopic survey. On the other hand, [2] published a reflectance spectrum suggesting that Phaethon does not belong to the F taxonomic class. As we extensively explained in a very recent paper [3], the investigations carried out by different authors, based on spectroscopic and dynamical evidence, has not been so far sufficient to draw definitive conclusions about the real nature of Phaethon.

2. Polarimetry as a useful tool

A very interestiong result of asteroid polarimetry is that the objects belonging to the old F-class display some unusual properties in their phase-polarization curve, which are sufficient to identify them as a separate class. In particular, the most important characteristic is a low value of the so-called inversion angle of polarization, that is the value of phase angle at which there is the transition from observing conditions in which the plane of linear polarization of the asteroid's light is found to be parallel to the Sun-observer-target plane (scattering plane) to observing conditions in which the plane of linear polarization is found to be normal to the scattering plane. Interestingly enough, the same property displayed by F-class asteroid has been found to be also exhibited by some cometary nuclei (see references in [3]. This opens the perspective of determining the physical nature of Phaethon (asteroid or comet) by means of an analysis of its phase- polarization curve. For this reason we organized a campaign of polarimetric observations of (3200) Phaethon during its last apparition in December 2017.

3. Results

We observed (3200) Phaethon in BVRI colours using the C2PU facilities of the Calern observing station of the observatory of Nice (France) and in R colour using the 2-m telescope of the Rhozen observatory (Bulgaria). Our polarimetric observations covered a very wide interval of phase angles, all of them belonging to the positive polarization branch, where the linear polarization plane is found to be normal to the scattering

plane. One should not that the high values of phase angle of our observations were made possible by the fact that Phaethon is a near-Earth asteroid, and could be observed when being at a short distance from the Earth, in a wide and rapidly changing interval of observing conditions.

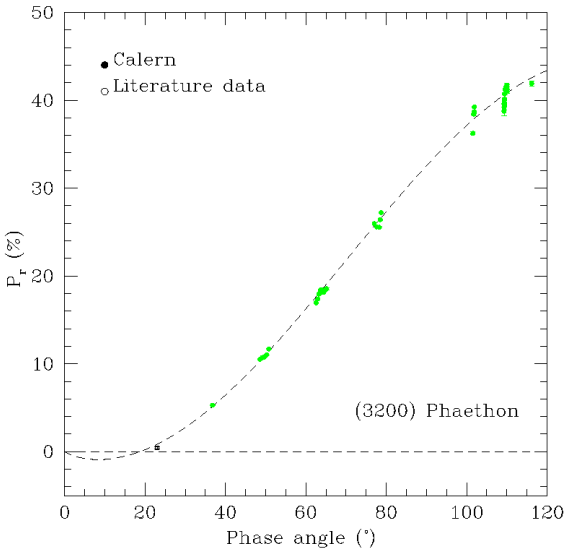

Figure 1: Phase - polarization curve of (3200) Phaethon in V light. The green symbols indicate the results of our measurements. One single previous measurement available in the literature is indicated by a black symbol.

The results of our observations can be summarized as follows:

1. We have measured the highest values of linear polarization ever found for objects of the solar system.

2. We derive an estimate of the P_{max} polarimetric parameter, namely the maximum value of polarization attained in the positive polarization branch. The obtained value suggests a very low value for the geometric albedo.

3. The phase - polarization curve of (3200) Phaethon seems to be poorly compatible with the F-class. Conversely, a much better agreement is found with the polarimetric properties of (2) Pallas. This confirms previous suggestions of [4] who suggested that Phaethon could be an evolved member of the Pallas' dynamical family.

4. Summary and Conclusions

We plan to obtain further polairmetric observations covering also the negative polarization branch during the next apparition of this asteroid. This will allow us to obtain definitive conclusions about its incompatibility with the polarimetric behaviour of the F-class, and its resemblance with the polairmetric properties of (2) Pallas.

Acknowledgements

The Torino polarimeter was built at the INAF - Torino Astrophysical Observatory using dedicated funds provided in the framework of the INAF PRIN 2009 program. This work is based on data obtained at the C2PU facility (Calern observing station, Observatoire de la Côte d'Azur, Nice, France) and at the Rozhen National Astronomical Observatory (Bulgaria). GB, ZD and YK gratefully acknowledge observing grant support from the Institute of Astronomy and Rozhen National Astronomical Observatory, Bulgarian Academy of Sciences.

References

[1] Tholen, D.J.: (3200) 1983 TB, IAU Circular 4034, 1985.

[2] Cochran A. L. and Barker E. S.: Minor planet 1983TB - A dead comet? Icarus, 59, 296-300, 1984.

[3] Devogèle, M. et al.: The phase - polarization curve of asteroid (3200) Phaethon, MNRAS, accepted, 2018.

[4] De León J., Campins H., Tsiganis K., Morbidelli A., Licandro J.: Origin of the near-Earth asteroid Phaethon and the Geminids meteor shower, A&A, 513, A26, 2010.

EPSC Abstracts
Vol. 12, EPSC2018-572, 2018
European Planetary Science Congress 2018

The Mission Accessible Near-Earth Objects Survey (MANOS): first results from the visible spectroscopic survey

Maxime Devogele (1), Nicholas Moskovitz (1), Cristina Thomas (2), Audrey Thirouin (1), Michael Mommert (1), David Polishook (3), Brian Skiff (1), Mitchell Magnuson (2), and Annika Gustafsson (2)
(1) Lowell Observatory, Flagstaff, AZ, USA , (2) Northern Arizona University, Flagstaff, AZ, USA, (3) Weizmann Institute of Science, Rehovot, Israel

Abstract

The Mission Accessible Near-Earth Objects Survey (MANOS) aims at characterizing sub-km, low delta-v, newly discovered Near-Earth Objects (NEOs). This survey, started in August 2013, is collecting astrometry, lightcurve photometry, and reflectance spectra of this under-studied portion of the NEO population. The MANOS program is using 1 to 8 meter telescopes located around the world. Here we present the first results of the visible reflectance spectroscopy survey obtained with the 8.1-meter Gemini North and South telescopes, the 4.3-meter Discovery Channel Telescope and the 4.1-meter SOAR telescope.

1. Introduction

Near-Earth objects (NEOs; defined by perihelia $<$1.3 AU) are small objects in the Solar System which regularly make close approaches with the Earth. For more than two decades these objects have been increasingly targeted for observations in photometry, spectroscopy, and radar ranging. These observations have provided valuable information about their physical characterization.

Scientifically, NEOs are essential to understand the formation and origin of the Solar System. They are the source of the meteorites, but assessing the link between them and NEO physical characteristics is not an easy task. The surface properties of NEOs are modified over time due to phenomena such as space weathering, and the meteorites examined on Earth have also undergone physical and chemical changes due to environmental weathering. In that sense, studying NEOs is essential to clarify these processes. Their full characterization (composition, size, density) is also of great importance in assessing defense strategies and damage previsions on the ground in the event of a potential impact. Lastly, NEOs are potential targets for in-situ resource utilization either for mining or life support for manned mission. They will be the subject of several spacecraft missions in the next decades (OSIRIS-REx, Hayabusa2, DART, DESTINY+)

The physical properties of NEOs seem to be size dependent. Whether or not these objects can be covered by regolith, or must be necessarily monolithic, is still an open question. Laboratory measurement have proven that grain size is an important parameter and could be responsible for variation in the slope or band depth [3, 2]. Compositional discrepancy is also observed between large NEOs (>1km) and meteorites [7, 10].

2. What is MANOS ?

The Mission Accessible Near-Earth Objects Survey (MANOS) started in August 2013 and is a multi-year survey supported by the National Optical Astronomy Observatory (NOAO) and Lowell Observatory, and funded by the NASA NEOO (Near-Earth Object Observations) office. The MANOS program consists of a physical characterization survey at visible and near-infrared wavelengths which is providing light-curves, astrometry, and reflectance spectra of sub-km, low delta-v (typically $<$7 km/s) NEOs. MANOS often targets newly discovered objects, which typically do not have a brighter apparition for the next several years or even decades. First MANOS results can be found in [8].

3. Data reduction

All spectroscopic data have been reduced using a new python based pipeline for long-slit spectroscopy reduction developed specifically for this project. This pipeline is intended to be easily portable to any visible spectrograph and is optimized for asteroid spectral reduction. The use of the same pipeline for all data obtained by this survey allows us to obtain a consistent data set of spectral properties of small NEOs. This

pipeline will be released as an open source package in the near future. An example of a reduced spectra can be see in Fig. 1

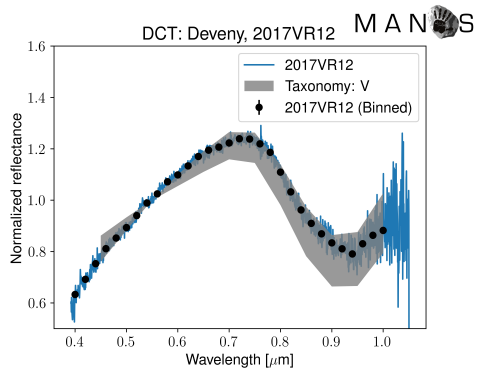

Figure 1: Example of spectrum obtained by the Deveny instrument from the 4.3m Discovery Channel Telescope (DCT).

4. Spectroscopic survey

We report here the first results of the visible spectroscopic survey of small NEOs. We have determined the taxonomic type of more than 300 asteroids with a mean size around 40 to 100 meters (H = 25) and as small as few meters (H=30). Fig. 2 shows the distribution of H magnitude of the NEOs observed by the MANOS project. This is the first comprehensive dataset of NEOs smaller than 100 meters with taxonomic type determined for each object. We will discuss the compositional properties of the NEO population (km and sub-km) [6, 9, 4], and how these populations compare to Main Belt asteroids [1, 5]. We will also compare the population of small NEOs with the meteorite population.

Acknowledgements

MANOS is funded by the NASA Near-Earth Object Observations program, grant number NNX17AH06G.

References

[1] Bus and Binzel 2002, Phase II of the Small Main-Belt Asteroid Spectroscopic Survey: A Feature-Based Taxonomy, Icarus, 146, 177

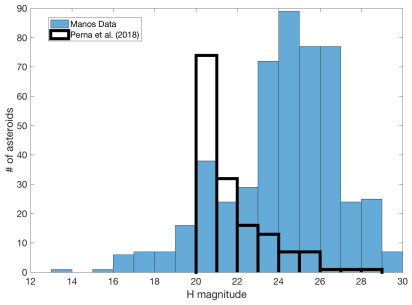

Figure 2: Distribution of H magnitude of the MANOS observed NEOs in spectroscopy compared to the data presented in Perna et al. (2018).

[2] Cloutis E. et al., Spectral reflectance properties of HED meteorites+ CM2 carbonaceous chondrites: Comparison to HED grain size and compositional variations and implications for the nature of low-albedo features on Asteroid 4 Vesta

[3] Cooper D. and Mustard J., 1999, Effects of Very Fine Particle Size on Reflectance Spectra of Smectite and Palagonitic Soil

[4] DeMeo F. and Binzel R.P., 2008, Comets in the near-Earth object population, Icarus, 194, 436

[5] DeMeo F. et al., 2009, An extension of the Bus asteroid taxonomy into the near-infrared, Icarus, 194, 436

[6] Perna D. et al., 2018, A spectroscopic survey of the small near-Earth asteroid population: peculiar taxonomic distribution and phase reddenig, accepted in Planetary and Space Science.

[7] Stuart J. and Binzel R.P., 2004, Bias-corrected population, size distribution, and impact hazard for the near-Earth object, Icarus, 170, 295

[8] Thirouin A. et al., 2016 The Mission accessible Near-Earth Object Survey - First Photometric Result, The Astronomical Journal, 152, 163.

[9] Thomas C. et al, 2011, ExploreNEOs. V. Average albedo by taxonomic complex in the Near-Earth asteroid population, The Astronomical Journal, 142, 85.

[10] Vernazza P. et al., 2008, Compositional differences between meteorites and near-Earth asteroid, Nature, 454, 858

EPSC Abstracts
Vol. 12, EPSC2018-730-1, 2018
European Planetary Science Congress 2018

Phase angle effects in brightness and polarization for different classes of small Solar system bodies

I. N. Belskaya (1) and V. G. Shevchenko (2,1)
(1) Institute of Astronomy, V. N. Karazin Kharkiv National University, Sumska Str. 35, Kharkiv 61022, Ukraine, (irina@astron.kharkov.ua) (2) Department of Astronomy and Space Informatics of V. N. Karazin Kharkiv National University, 4 Svobody Sq., Kharkiv 61022, Ukraine (shevchenko@astron.kharkov.ua)

Abstract

We review the available observational data on magnitude and polarization phase angle dependences of small Solar system bodies from different dynamical groups, including Near-Earth objects, main belt asteroids, Trojans, Centaurs, and transneptunian objects (TNOs). Diversities and similarities in phase angle behaviours of atmosphereless small bodies orbiting at different distances from the Sun are discussed. We focus on observed correlation of phase curve parameters with albedo and interrelations between photometric and polarimetric phase curve characteristics.
.

1. Introduction

Study of phase angle effects in brightness and polarization of atmosphereless Solar system bodies give a first look into top-most surface properties. A sharp increase in brightness and the negative branch in the degree of linear polarization are common phenomena observed at small phase angles for different types of Solar system bodies. Both phenomena are considered to have similar physical nature and their joint analysis is of a great value to better understand light-scattering mechanisms and to improve basis for data interpretation in terms of physical characteristics of the surface regoliths.

2. Results

For main-belt asteroids a strong correlation was found between the linear slope of magnitude-phase dependences defined in the range of 5–25° and the geometric albedo [1]. A twofold increase in the amount of high-quality observational data has confirmed strong albedo dependence of the phase slope (Fig.1). An existence of such correlation suggests that albedo is the main factor influencing the slope of main-belt asteroid phase curves (at least up to 25°).

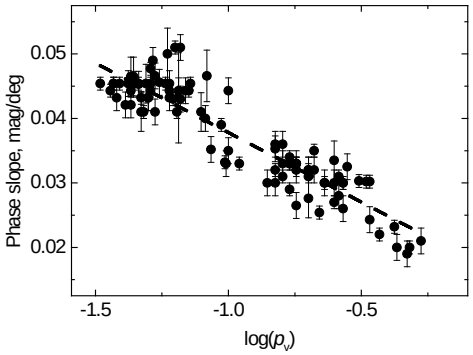

Figure 1: Correlation between slope of asteroid phase curves and albedo.

The value of opposition effect amplitude (defined as an excess in magnitude relatively to linear approximation of phase curve at zero phase angle) depends on albedo in more complicated way (Fig.2).

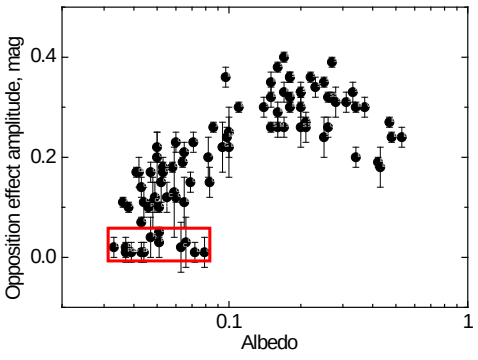

Figure 2: Dependence of the opposition effect amplitude of asteroids on albedo. Several asteroids (in the red rectangle) have not revealed non-linear opposition surge.

Some of low-albedo asteroids show linear phase-angle magnitude dependences down to very small phase angles. The only plausible explanation of such effect is an assumption of extremely low surface albedo of asteroids not showing opposition effect [2]. These asteroids belong mainly to the primitive P and D types. Moreover, magnitude-phase dependences of the P-type asteroids belonging to the main belt, Hilda and Cybele groups, and Trojans are found to be indistinguishable within the errors of measurements [3, 4]. Phase curves of Centaurs measured at small phase angles differ from those for asteroids and show greater diversity. For TNOs a very narrow opposition effect is inherent [5].

The parameters characterizing brightness opposition effect and negative polarization branch have a tendency to correlate. The negative polarization branch of low albedo asteroids becomes less deep when the opposition effect amplitude decreases. Correlations of polarimetric parameters with albedo are successfully used for asteroid albedo determinations (see e.g. [6]). That is not the case for TNOs and Centaurs for which correlation between polarization and albedo is rather weak [7]. The distinct feature of their polarization behavior is a pronounced negative polarization at small phase angles (except for largest dwarf planets). Their polarization minimum is shifted toward small phase angles as compare to main-belt asteroids and Jupiter Trojans [8].

3. Conclusions

The magnitude and polarization phase angle dependences measured for different classes of small Solar system bodies revealed many interesting features and interrelationships. Their interpretation in terms of physical parameters of surface properties is still in progress. The measured observational features need to be taking into account to improve theoretical models of lightscattering by planetary surfaces.

References

[1] Belskaya, I.N., and Shevchenko, V. G. 2000. Icarus 146, 490-499.

[2] Belskaya, I.N., and Shevchenko, V. G. 2017. Extremely dark asteroids. Abstr. for Asteroids, Comets, Meteors 2017, Montevideo, Uruguay, p. 596.

[3] Shevchenko, V. G., et al. 2012. Icarus 217, 202–208.

[4] Slyusarev, I. G., et al. 2012. Magnitude phase angle dependences of Jupiter Trojans and Hilda asteroids. 43rd Lunar and Planetary Science Conference, No. 1659, p. 1885.

[5] Belskaya, I.N., Levasseur-Regourd, A.-C., Shkuratov, Yu.G., Muinonen, K. 2008. Surface properties of Kuiper-Belt objects and Centaurs from photometry and polarimetry. In: The Solar System Beyound Neptune (Barucci, A., et al., Eds.), Univ. of Arizona Press, p. 115-127.

[6] Cellino, A., et al. 2015. On the calibration of the relation between geometric albedo and polarimetric properties for the asteroids. MNRAS 451, p.3473-3488.

[7] Belskaya, I.N., and Bagnulo, S. 2015. Polarimetry of transneptunian objects and centaurs. In: Polarimetry of stars and planetary systems (L. Kolokolova, A.-C. Levasseur-Regourd, J. Hough, eds.), Cambridge University Press, p. 405-418.

[8] Bagnulo, S., et al. 2015. Broadband linear polarization of Jupiter Trojans. Astron. Astroph. 585, id.A122, 12 p.

EPSC Abstracts
Vol. 12, EPSC2018-761-1, 2018
European Planetary Science Congress 2018

Asteroid photometric phase curves from Gaia observations

Karri Muinonen (1,2), Maria Gritsevich (1), and Alberto Cellino (3)

(1) Department of Physics, University of Helsinki, Finland (karri.muinonen@helsinki.fi) (2) Finnish Geospatial Research Institute FGI, Masala, Finland, (3) INAF, Osservatorio Astrofisico di Torino, Pino Torinese, Italia

Abstract

The photometric phase curve of an asteroid refers to the dependence of disk-integrated brightness on the phase angle (the Sun-Object-Observer angle). In the present work, we study the feasibility of constraining asteroid phase curve parameters from the sparse photometry available from Gaia Data Release 2. An asteroid's lightcurve, i.e., its observed disk-integrated brightness as a function of time, depends on the shape and spin state of the asteroid, as well as its surface scattering properties. It follows that these properties can be estimated from the observations, to an extent allowed by a given data set. In order to facilitate the rapid assessment of the phase curves, we utilize the so-called Lommel-Seeliger ellipsoids in the statistical inversion of Gaia photometry. We transform the resulting phase curves to reference equatorial illumination and observation of the given asteroid. These reference phase curves can have substantial value in asteroid taxonomy.

1. Introduction

Asteroids are irregularly shaped Solar System bodies typically rotating about their axes of maximum inertia. Their surfaces are typically covered by regoliths, that is, by layers of particulate material in the size scales of microns to meters, with the typical particle size being of the order of 100 microns. Asteroids offer information about the evolution of the Solar System, provide valuable space resources, and cause an impact hazard for life on the Earth.

The most common source of data on the asteroids is photometry: the measurement of the disk-integrated brightness of the asteroid. An asteroid's lightcurve, i.e., its observed brightness as a function of time, depends on the shape and spin state of the asteroid, as well as its scattering properties. In the present work, we consider sparse photometric data from the ESA Gaia mission made available by Gaia Data Release 2 (Gaia DR2, [1]). We utilize statistical inverse methods for the retrieval of rotation periods, pole orientations, and scattering properties from the photometric observations. This entails a complete Markov chain Monte Carlo assessment of the uncertainties in the physical parameters. The inverse methods are based on the Lommel-Seeliger ellipsoids [2-5] suitable for the analyses of sparse data. The computational tools based on the present inverse methods are available through a web-based Gaia Added Value Interface [6].

2. Results and discussion

We have validated the Gaia photometric data by using high-resolution shape models of (21) Lutetia [7] and (2867) Steins [8]. Figure 1 shows an example of the validation for (21) Lutetia. Typically, the Gaia photometric data can be validated with numerical modeling at a root-mean-square difference level (RMS) of 0.01-0.02 magnitudes. We would like to point out that a large part of the RMS difference is likely to derive from the modeling: the Gaia data can have significantly smaller uncertainties.

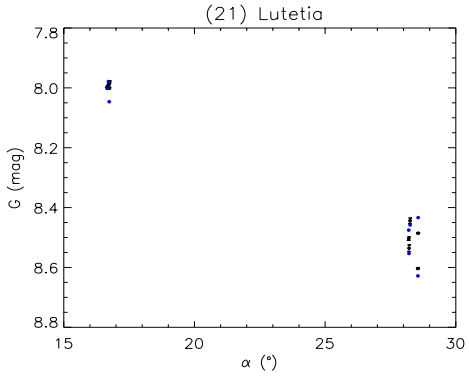

Figure 1: Photometry of asteroid (21) Lutetia from Gaia Data Release 2 (black dots) validated using a high-resolution shape model (blue dots, [7]) with a Lommel-Seeliger scattering law [2] reproducing the phase curve from ground-based observations [9].

We will carry out a systematic study of the Gaia DR2 asteroid photometry to estimate the parameters of the H, G_1, G_2 photometric function [10-12]. In doing so, we may be obliged to invoke informative a priori probability densities on the physical parameters, making the statistical inverse problem highly challenging.

3. Conclusion

We conclude that the present inverse methods can facilitate a meaningful phase curve retrieval from sparse Gaia DR2 photometry.

4. Acknowledgments

Research supported, in part, by the ERC Advanced Grant 320773.

References

[1] Gaia Collaboration, Spoto, F., et al. Astron. Astrophys., in press, 2018.

[2] Muinonen, K., and Lumme, K. (2015). Disk-integrated brightness of a Lommel-Seeliger scattering ellipsoidal asteroid. Astron. Astrophysics 584, A23, 2015.

[3] Cellino, A., Muinonen, K., Hestroffer, D., and Carbognani, A.: Inversion of sparse photometric data of asteroids using triaxial ellipsoid shape models and a Lommel-Seeliger scattering law. Planet. Space Sci., 118, pp. 221-226, 2015.

[4] Muinonen, K., Wilkman, O., Cellino, A., Wang, X., and Wang, Y.: Asteroid lightcurve inversion with Lommel-Seeliger ellipsoids. Planet. Space Sci., 118, pp. 227-241, 2015.

[5] Muinonen, K., Torppa, J., Gritsevich, M., Wang, X., Cellino, A. Asteroid lightcurve inversion with Bayesian inference. Astron. Astrophys., in preparation, 2018.

[6] Torppa, J., Granvik, M., Penttilä, A., Reitmaa, J. Tudose, V., Pelttari, L., Muinonen, K., Bakker, J., Navarro, V., O'Mullane, W. Added-value interfaces to asteroid photometric and spectroscopic data in the Gaia database. Adv. Space Res., in press, 2018.

[7] Sierks, H., et al. Images of asteroid 21 Lutetia: A remnant planetesimal from the early solar system. Science 334, pp. 487-490, 2011.

[8] Jorda, L., Lamy, P. L., Gaskell, R. W., Kaasalainen, M., Groussin, O., Besse, S., Faury, G. Asteroid (2867) Steins: Shape, topography and global physical properties from OSIRIS observations. Icarus 221, pp. 1089-1100, 2012.

[9] Belskaya, I. N., Fornasier, S., Krugly, Yu. N., Shevchenko, V. G., Gaftonyuk, N. M., Barucci, M. A., Fulchignoni, M., and Gil-Hutton, R. Puzzling asteroid 21 Lutetia: our knowledge prior to the Rosetta fly-by. Astron. Astrophys. 515, A29, 2010.

[10] Muinonen, K., Belskaya, I. N., Cellino, A., Delbò, M., Levasseur-Regourd, A.-C., Penttilä, A., and Tedesco, E. F. A three-parameter magnitude phase function for asteroids. Icarus 209, pp. 542-555, 2010.

[11] Penttilä, A., Muinonen, K., Shevchenko, V. G., and Wilkman, O. H, G_1, G_2 photometric phase function extended to low-accuracy data. Planet. Space Sci. 123, pp. 117-125, 2016.

[12] Shevchenko, V. G., Belskaya, I. N., Muinonen, K., Penttilä, A., Krugly, Y. N., Velichko, F. P., Chiorny, V. G., Slyusarev, I. C., Gaftonyuk, N. M., and Tereschenko, I. A. Asteroid observations at low phase angles. IV. Average parameters for the new . H, G_1, G_2 magnitude system. Planet. Space Sci. 123, pp. 101-116, 2016.

EPSC Abstracts
Vol. 12, EPSC2018-762, 2018
European Planetary Science Congress 2018

Wavelength-dependent multiple scattering modeling for planetary regoliths

Johannes Markkanen (1), Timo Väisänen (2), Jessica Agarwal (1), Antti Penttilä (2), and Karri Muinonen (2,3)
(1) Max Planck Institute for Solar System Research, Göttingen, Germany, (2) Department of Physics, University of Helsinki, Finland, (3) Finnish Geospatial Research Institute FGI, Masala, Finland. (markkanen@mps.mpg.de)

Abstract

We present a computational approach for modeling light scattering and absorption in planetary regoliths composed of densely packed particles. The approach is based on the rigorous electromagnetic theory hence it allows for a quantitative analysis of photometric and polarimetric observations of airless planetary bodies. We will model and compare the photometric and polarimetric phase functions of typical asteroids and the surface of comet 67P/Churyumov-Gerasimenko.

1. Introduction

Interpretation of remote light scattering observations of small bodies in the Solar System relies on numerical modeling. Surfaces of small bodies such as asteroids and comets are covered by small dust particles, that is, planetary regolith. Solving light scattering characteristics of such surfaces is not an easy task. First, particle sizes are of the order of the wavelength of incident light, meaning that one has to consider the wave nature of light described by Maxwell's equations. Second, the particles are not spherical, and third, the entire body is large compared to the wavelength which renders the exact electromagnetic solvers inapplicable.

Large numbers of different approximate models exist that are loosely based on the radiative transfer equation, e.g., the Hapke model. The model parameters, however, are not directly linked to the physical properties of the target [1]. Further, the standard radiative transfer approach does not work for media composed of densely packed particles. For the quantitative interpretation of light scattering observations of planetary regoliths, rigorous and efficient numerical methods are needed.

Recently, we have developed a numerical method based on the rigorous multiple scattering theory, called as radiative transfer with reciprocal transactions (R^2T^2) [2, 3], which allows us to close the gap between the exact solutions for microscopic particles and the approximate solutions for macroscopic objects. Thus, we can build a chain of numerical solvers that provide a realistic model for light scattering and absorption in planetary regoliths. In this work, we demonstrate that these methods can be used to interpret spectropolarimetric and photometric observations of planetary regoliths.

2. Numerical methods

Modeling electromagnetic scattering by planetary regoliths is a multiscale scattering problem involving microscopic and macroscopic details. Thus, not a single numerical method can solve such a problem alone, but we need to combine different methods in a hierarchical manner. Figure 1 illustrates different numerical solvers and the particle size range in which each method is applicable at visible wavelengths.

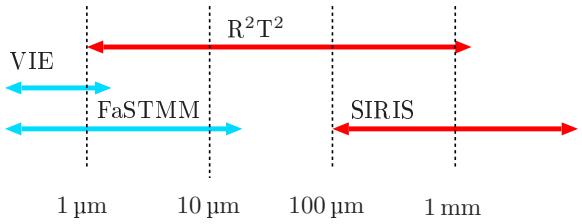

Figure 1: The range of applicability for different numerical methods is shown. The blue lines denote the exact numerical methods and the red lines denote the approximate methods. In order to solve scattering by planetary regoliths, the methods are used in a hierarchical manner.

2.1 Exact methods

Exact numerical methods such as the volume integral equation (VIE) method and the fast superposition T-matrix method (FaSTMM) solve Maxwell's equations exactly without any physical approximation [4]. The

drawback is that they are computationally expensive, and in practice, they cannot be applied for large objects. Here we use the exact method to compute input data to the R^2T^2 method.

2.2 Approximate methods

The R^2T^2 method is based on the order-of-scattering (OOS) representation of the electric field. We formulate the OOS solution for the clusters of particles (volume elements) rather than the single particles allowing us to find the solution for a scattering problem involving densely packed particle systems. To solve the OOS equation, we apply a Monte Carlo algorithm in which each scattering sequence is computed exactly with the FaSTMM. Thus, we can treat large media consisting of arbitrarily shaped and inhomogeneous particles. The method, however, cannot treat macroscopic surface roughness, hence as a final step, we use the output of the R^2T^2 as input for the SIRIS solver [5]. The SIRIS solver is a Monte Carlo radiative transfer solver coupled with geometric optics that can take macroscopic surface roughness into account.

3. Numerical example

We consider scattering by 1-cm sized porous particle (porosity = 0.75) consisting of iron-rich silicate grains ($m = 1.7 + \mathrm{i}0.03$) of size 0.4 ± 0.1 microns at $\lambda = 649$nm. Such material compositition is typical for S-type asteroids. Figure 2 shows the Mueller matrix element S11 normalized to the geometric albedo and the degree of linear polarization -S_{12}/S_{11} for two different types of small grains, irregular and spherical.

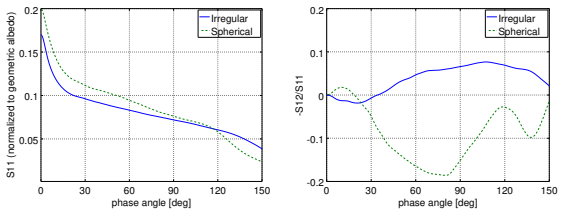

Figure 2: Computed intensity and the degree of linear polarization for the 1-cm sized iron-rich silicate particle consisting of densely packed irregular or spherical grains.

The polarization phase curve demonstrates the importance of using non-spherical particles as constituent grains of the medium. Resonances associated with the spherical shapes are clearly visible. With irregular grains the resonances vanish and the polarization curve is more consistent with observations, i.e., showing a bell-shaped polarization curve with a negative branch at low phase angles and the maximum positive polarization near 90 degrees.

4. Conclusions

We have presented a novel numerical method for modeling light scattering and absoption in planetary regoliths. The method allows for a quantitative interpretation of photometric and polarimetric observations of airless planetary bodies such as asteroids, moons, and comets.

References

[1] Shkuratov, Y., Kaydash, V., Korokhin, V., Velikodsky, Y., Petrov, D., Zubko, E., Stankevich, D., Videen, G., A critical assessment of the Hapke photometric model, JQSRT, vol. 113, 2431–2456, 2012.

[2] Muinonen, K., Markkanen, J., Väisänen, K., Peltoniemi, J., Penttilä, J., Multiple scattering of light in discrete random media using incoherent interactions, Opt. Lett., vol. 43, 683–686, 2018.

[3] Markkanen, J., Väisanen, T., Penttilä, A., and Muinonen, K. Scattering and absorption in dense discrete random media of irregular particles, Opt. Lett., 2018, accepted.

[4] Markkanen, J., and Yuffa, A.J., Fast superposition T-matrix solution for clusters with arbitrarily-shaped constituent particles, JQSRT, vol. 189, 181–188, 2017.

[5] Muinonen, K., Nousiainen, T., Lindqvist, H., Muñoz, O., and Videen, G., Light scattering by Gaussian particles with internal inclusions and roughened surfaces using ray optics. JQRST, vol. 110, 1628–1639, 2009.

EPSC Abstracts
Vol. 12, EPSC2018-836, 2018
European Planetary Science Congress 2018

First steps towards a database of polarisation spectra of asteroids

Stefano Bagnulo (1), Alberto Cellino (2), Galin Borisov (1), Apostolos Christou (1), Daphne Stam (3), Irina Belskaya (4), Michael Sterzik (5) and Karri Muinonen (6,7) (1) Armagh Observatory & Planetarium, Armagh, UK (stefano.bagnulo@armagh.ac.uk, galin.borisov@armagh.ac.uk, apostolos.christou@armagh.ac.uk), (2) INAF - Osservatorio Astrofisico di Torino, Pino Torinese, Italy (alberto.cellino@inaf.it) (3) Faculty of Aerospace Engineering, Delft University of Technology, Delft, The Netherlands (D.M.Stam@tudelft.nl), (4) Institute of Astronomy, V.N. Karazin Kharkiv National University, Kharkiv, Ukraine (irina@astron.kharkov.ua) (5) ESO, Garching bei Muenchen, Germany (msterzik@eso.org), (6) Department of Physics, University of Helsinki, Finland, (7) National Land Survey of Finland, Finnish Geospatial Research Institute, Helsinki, Finland

Abstract

We have collected polarisation spectra for over 70 asteroids of various taxonomic classes. Data obtained so far confirm a predictable relation between polarization spectra and albedo, but at the same time indicate also some previously unexplored dependences upon other surface properties, including regolith properties. We show that asteroids exhibiting very similar reflectance spectra can display strong differences in their polarization spectra, and we conclude that spectropolarimetry is a more powerful tool to reveal the great diversity displayed by the small bodies of our solar system than traditional spectro-photometric techniques.

1. Introduction

Light scattered by surfaces is polarized. The state of the polarization of the scattered radiation depends on the structure and composition of the reflecting surface and on the scattering angle, and polarimetric measurements as function of the scattering angle may reveal information about the physical properties of the reflecting surface.

Broadband linear polarization (BBLP) measurements have long been used as a remote sensing tool for the characterisation of the objects of our solar system. BBLP measurements in the standard optical filters are usually plotted as a function of the phase-angle (the angle between the sun and the observer as seen from the target object). The morphology of the resulting phase-polarization curves may be used for the purposes of albedo determinations (see Cellino et al. 2015 and references therein), to infer some properties of the surface regolith such as the average particle sizes, and for asteroid classification (Penttilä et al. 2005, Belskaya et al. 2017).

Comparatively less attention has been paid to the way polarisation depends on wavelength. Most of the relevant works are actually based on multi-filter BBLP measurments (Lupishko & Kiselev 1995; Belskaya et al. 2009; Lupishko & Shkuratov 2016) while low-resolution spectropolarimetry of asteroids was introduced by Bagnulo et al. (2015).

2. Earlier works

Bagnulo et al. (2015) have shown that polarization spectra of low albedo and intermediate albedo asteroids exhibit opposite trends, namely: the polarization spectra of low albedo asteroids always have a positive gradient, and intermediate albedo asteroids always have a negative gradient. This confirmed preliminary results obtained by Lupishko & Kiselev (1995) and Belskaya et al. (2009), based on multi-colour BBLP data, and suggested that the slope of the polarization spectra may be linked to the albedo. Bagnulo et al. (2015) also unveiled an unexpected variety of situations. Some of them show up as violation of the Umov law. The Umov law says that light reflected by darker objects is more polarized than light reflected by objects with higher albedo; however, it was found that in contrast to what expected from basic physical considerations, reflectance and polarization spectra of asteroid (236) Honoria are correlated positively. This discovery represents a challenge for theory, and stimulates further developments of the modelling of the scattered light. Both Belskaya et al. (2009) and Bagnulo et al. (2015) proposed that the slope of the spectral dependence of polarization of asteroids exhibit opposite signs in the negative and in the positive branch

of the curve of polarisation versus phase-angle. This fact was confirmed (on a more systematic basis) by Lupishko & Shkuratov (2016).

If we could establish a firm link between albedo and wavelength-dependence of the degree of polarization (as our preliminary results seem to suggest) we would accomplish a crucial step forward in asteroid science: joint to absolute magnitude measurements, spectropolarimetry would allow us to measure the size of asteroids, with implications particularly important for the characterization of potentially hazardous near-Earth objects.

3. New measurements

Using the ISIS instrument of the William Herschel Telescope and the FORS2 instrument of the ESO Very Large Telescope, we have now collected 144 polarisation spectra of 72 different asteroids belonging to different taxonomic classes and with different albedo, and started to construct the first spectropolarimetric database of asteroids. We have explored in detail the complex taxonomic classes S and C, which include a significant numbers of sub-classes that can correspond to a variety of relevant differences in terms of composition, regolith properties and overall collisonal and thermal histories of the objects. While still working on a classification scheme for spectropolarimetry, we have found examples of asteroids with relatively similar optical reflectance spectra but different polarization properties. The natural interpretation of this finding is that the diversity of surface structures may best revealed via spectropolarimetric measurements than through "usual" spectro-photometry.

Acknowledgements

This research is based on observations collected at the Very Large Telescope of the ESO La Silla-Paranal Observatory, and at the William Herschel Telescope of the Isaac Newton Group of telescopes.

References

[1] Bagnulo, S., Cellino, A., Sterzik. M.F.: Linear spectropolarimetry: a new diagnostic tool for the classification and characterization of asteroids, Monthly Notices of the Royal Astronomical Society, Vol. 446, pp. L11-L15, 2015.

[2] Cellino, A., Bagnulo, S., Gil-Hutton, R., Tanga, P., Cañada-Assandri, M., Tedesco, E.F.: On the calibration of the relation between geometric albedo and polarimetric properties for the asteroids, Monthly Notices of the Royal Astronomical Society, Vol. 451, pp. 3473-3488, 2015.

[3] Belskaya, I.N., Levasseur-Regourd, A.-C., Cellino, A., Efimov, Y.S., Shakhovskoy, N.M., Hadamcik, E., Bendjoya, P.: Polarimetry of main belt asteroids: Wavelength dependence, Icarus, Vol. 199, pp.97-105, 2009.

[4] Belskaya, I.N., Fornasier, S., Tozzi, G.P., Gil-Hutton, R., Cellino, A., Antonyuk, K., Krugly, Yu.N., Dovgopol, A.N., Faggi, S.: Refining the asteroid taxonomy by polarimetric observations, Icarus, Vol. 284, pp. 30-42, 2017.

[5] Lupishko, D. F., Kiselev, N. N.: Inversion Effect of Spectral Dependence of Asteroid Polarization, Bulletin of the American Astronomical Society, Vol. 27, p. 1064, 1995.

[6] Lupishko, D. F., Shkuratov, Yu. G.: On spectral dependence of polarization of asteroids, Solar System Research, Vol. 50, pp. 329-336, 2016.

[7] Penttilä, A., Lumme, K., Hadamcik, E., Levasseur-Regourd, A.-C.: Statistical analysis of asteroidal and cometary polarization phase curves, Astronomy and Astrophysics, Vol. 432, pp. 1081-1090, 2005

EPSC Abstracts
Vol. 12, EPSC2018-1016, 2018
European Planetary Science Congress 2018

Linear polarisation of comets observed with STEREO

Rok Nezic (1,2,3), Stefano Bagnulo (1), Geraint H. Jones (2,3) and Galin Borisov (1,4)
(1) Armagh Observatory and Planetarium, UK (rok.nezic@armagh.ac.uk), (2) Mullard Space Science Laboratory, University College London, UK, (3) The Centre for Planetary Sciences at UCL/Birckbeck, UK, (4) Institute of Astronomy and National Astronomical Observatory, Sofia, Bulgaria

Abstract

The Lyot coronographs on the twin STEREO spacecraft observe the vicinity of the Sun in the 650-750 nm wavelength range. As well as solar physics, they have been well-utilised for comet hunting. Unlike most similar instruments, STEREO coronographs have a polariser permanently mounted in their optical path, which means full polarimetric analysis can be performed on large datasets of comet passages. Although the integration time is short and the signal is usually dominated by solar activity, polarimetric analysis of bright comets and their tails can be performed. If the geometry of the cometary encounter is favourable, a wider range of phase angles - particularly those above 90° - may be observed with solar-observing instruments than with other methods. We developed an improved method for polarimetric analysis of comets with known orbital elements observed with the STEREO spacecraft coronographs. The method reduces triplets of polarised images and calculates the degree of polarisation of the comet along its dust tail, with considerations of 3-D geometry, producing a phase angle curve. While most observed comets do not appear to survive the perihelion passage, a variety of polarisation properties has been observed. The method has shown to be robust and may also be extended to other solar observatories (e.g. SOHO).

1. Introduction

The STEREO spacecraft (**S**olar **Te**rrestrial **Re**lations **O**bservatory) mission is a pair of near-identical solar observatories (STEREO-A or Ahead and STEREO-B or Behind) launched in 2006 in heliocentric orbits lagging behind (STEREO-B) or advancing ahead (STEREO-A) of the orbit of the Earth. While its main focus is the 3-D analysis of the solar environment, the mission - like the earlier SOHO (**So**lar and **H**eliospheric **O**bservatory) mission [1] - has been successful at detecting near-Sun comets [4].

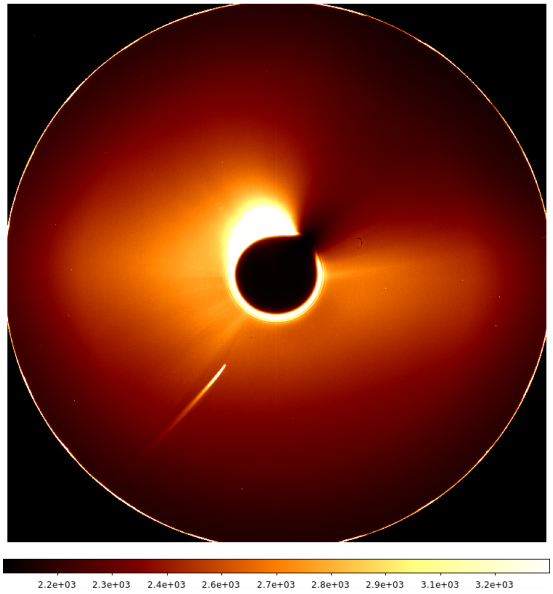

Figure 1: Comet C/2011 W3 (Lovejoy) as observed by STEREO-A/SECCHI/COR2 on 15th December 2011.

The most useful comet-hunting instruments aboard STEREO are in the SECCHI (**S**un-**E**arth **C**onnection **C**oronal and **H**eliospheric **I**nvestigation) suite of telescopes, which include two Lyot coronographs: COR1 (field of view $1.3 - 4.0 R_\odot$) and COR2 (field of view $2 - 15 R_\odot$) [3]. While SOHO has been more prolific in its discoveries of new comets than any other mission, including STEREO [1], the great advantage of the latter over the former is that the COR1 and COR2 instruments boast a rotatable polariser permanently positioned in their optical path. This allows for near-continuous polarimetric observations, which is particularly useful when observing the swiftly-moving near-perihelion comets. Another unique advantage of the STEREO mission is the relative positioning of the twin spacecraft (prior to 2014, when contact with STEREO-B was lost), meaning that comets have often been observed by both simultaneously. This not only

increases the amount of available data, but often also the range of observed phase angles.

The polariser angles for COR1 and COR2 coronographs are 0, 120, and 240°. They both observe within the wavelength passband of 650-750 nm, which excludes the dimmer comets when compared to SOHO. Stokes Q and U, as well as the degree of polarisation P, can be computed from these three orientations.

2. Methodology

The data reduction process we developed is similar on the one used by [5], with significant adaptations and generalisations, and using some routines from the SolarSoft library [2].

Notably, while [5] required the comet to be visible in both spacecrafts' fields of view to triangulate the three-dimensional position of the comet and its tail, a simplifying assumption allows the extraction of all relevant data from a single spacecraft with minimal loss of accuracy. Using either the calculated orbital elements or the vector products of multiple heliocentric positions of the comet, the normal to the cometary orbital plane can be determined. Assuming the dust tail remains in the orbital plane of the comet and using the position information of the spacecraft, we can project every point in a STEREO image to the cometary orbital plane and thus obtain the full three-dimensional information about it.

A triplet of images in each of the polarising angles is taken in rapid succession every hour, or more frequently in some early observations. These triplets are analysed and recombined to determine the polarisation of the comet (see Figure 1 for an example raw image).

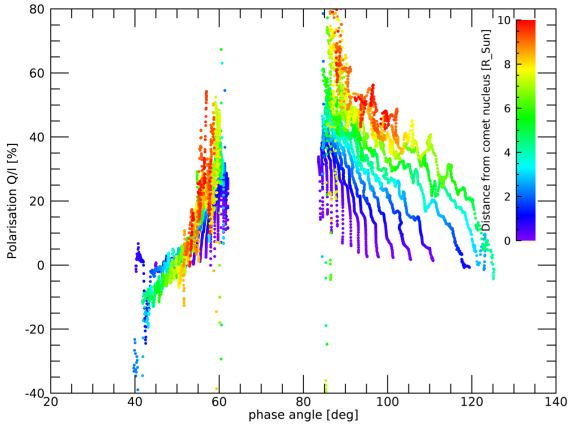

Figure 2: Phase curve of Comet C/2011 W3 (Lovejoy) during its December 2011 perihelion.

3. Results and Conclusions

To prove the accuracy of the new method, we first analysed the observations of comet C/2011 W3 (Lovejoy) and compared our results with [5], showing good agreement (see Figure 2 and compare it to Figure 9 within [5]). We then narrowed down a list of over 30 comets observed with COR2 to those bright enough for meaningful analysis. Results of this analysis will be presented here. They show our method can successfully reduce the STEREO images and provide us with polarimetric information on the comet, given a high enough signal-to-noise ratio. Phase curves can be plotted and compared to the literature, and variation of polarisation along the comet tail analysed.

STEREO-A and B spacecraft have a number of advantages which make them good candidates for polarimetric analysis of comets. Although only bright comets make good STEREO candidates, observations from STEREO and other solar observatories, for which our method can be adapted, can help expand our knowledge of polarisation of comets, and therefore of origin and evolution of comets at large.

Acknowledgements

We would like to thank R. Kracht for providing a detailed list of comets seen with STEREO/SECCHI, as well as M. Knight, K. Battams, V. Andretta for their help and collaboration. This research is supported through the United Kingdom Science and Technology Facilities Council.

References

[1] Battams, K. and Knight, M. M.: SOHO comets: 20 years and 3000 objects later, Phil. Trans. R. Soc. A, Vol. 375, 20160257, 2017

[2] Freeland, S. L. and Handy, B. N.: Data Analysis with the SolarSoft System, Solar Physics, Vol. 182, pp. 497-500, 1998

[3] Howard, R. A., Moses J. D., and Socker D. G.: Sun Earth Connection Coronal and Heliospheric Investigation (SECCHI), Proceedings of SPIE, Vol. 4139-26, 2000

[4] Jones, G. H., Knight, M. M., Battams, K. et al.: The Science of Sungrazers, Sunskirters, and Other Near-Sun Comets, Space Sci Rev, Vol. 214: 20, 2018

[5] Thompson, W. T.: Linear polarization measurements of Comet C/2011 W3 (Lovejoy) from STEREO, Icarus, Vol. 261, pp. 122-132, 2015.

EPSC Abstracts
Vol. 12, EPSC2018-1037, 2018
European Planetary Science Congress 2018

Light scattering from densely packed irregular particle clusters in the geometric optics regime using inhomogeneous waves

Timo Väisänen (1), Johannes Markkanen (2), Julia Martikainen (1), Hannakaisa Lindqvist (3), and Karri Muinonen (1,4)
(1) Department of Physics, University of Helsinki, Finland (2) Max Planck Institute for Solar System Research, Göttingen, Germany, (3) Finnish Meteorological Institute, Helsinki, Finland (4) Finnish Geospatial Research Institute FGI, Masala, Finland (timo.h.vaisanen@helsinki.fi)

Abstract

We simulate huge discrete random media composed of Gaussian random particles of different sizes and shapes in the geometric optics (GO) regime. The code used is an extended version of the SIRIS4, and supports multiparticle systems and inhomogeneous waves. This helps us to understand how the properties of the particles affect the output of the simulation, e.g. is there any size dependency, and helps us to improve shadowing functions and thus asteroid phase curve models.

1. Introduction

Simulating light scattering from a huge discrete random medium with exact methods such as the Volume integral equation solver or the Superposition T-matrix method is a challenge [1]. The required computational resources are even more tremendous, if the particles are larger than the wavelength ($\lambda \gg r$), but fortunately, in this region, geometric optics (GO) can be applied.

In the GO, electromagnetic waves are treated as rays, which can be traced individually in the studied system. SIRIS4 [2, 3] is an GO code, which has been successfully applied to spectral modeling [4]. The problem is that the code does not support multiparticle systems, but this will be fixed in the SIRIS4.1.

The new version can be applied to the discrete random media composed of Gaussian random particles such as shown in Fig. 1. The intensity and polarization curves from these simulations will help us to develop better understanding of how the geometry of the single particles will affect the overall light-scattering characteristics of the system.

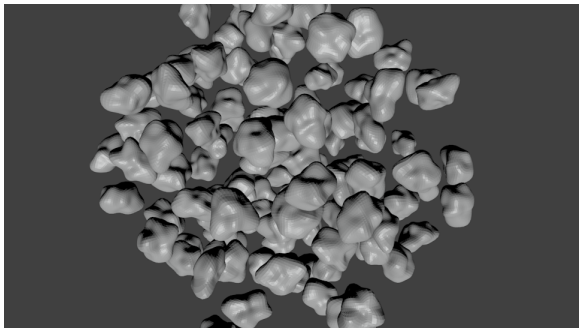

Figure 1: A discrete random medium composed of Gaussian random particles.

2. SIRIS4.1

SIRIS4.1 is a spin-off project from the original SIRIS4, which computed light-scattering characteristics of single particles by generating Gaussian random particles and tracing rays inside the particle. SIRIS4.1 supports ray tracing in dense random media with a huge number of particles.

As a preliminary result, Figs. 2 and 3 are shown. In these figures the GO and the radiative transfer (RT) were compared by simulating spherical discrete random media of packing density 10% and size parameter $kR = 5100$ made of $kr = 100$ particles. Both intensity (Fig 2) and polarization (Fig 3) were studied. These results were computed with a single computing core so there is a possibility to simulate even larger systems.

3. Summary

We will study discrete random media made of Gaussian random particles of different sizes and shapes in the geometric optics regime. In order to be able to do this, SIRIS4.1 needs to be finished with a proper

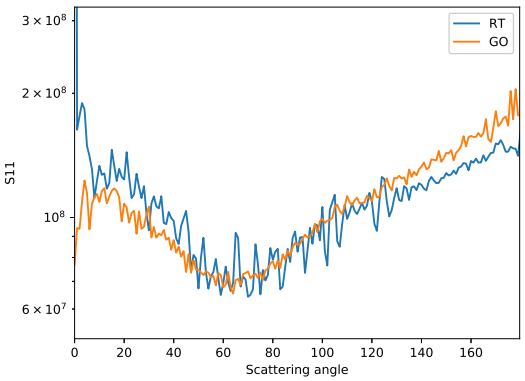

Figure 2: Intensity as a function of scattering angle.

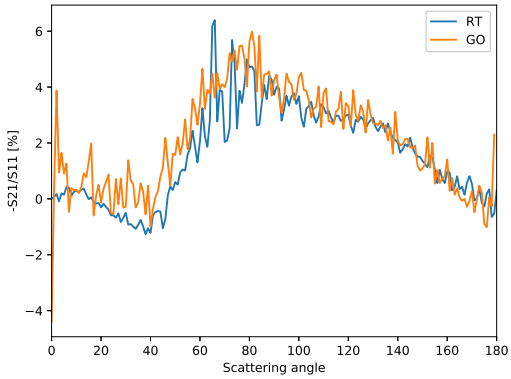

Figure 3: Degree of linear polarization as a function of scattering angle.

packing algorithm, which can support multiple irregular particles. The results will help us to understand how the features of a single particle can affect the output of the light scattering simulation. This knowledge can be then applied to improve asteroid phase curve models.

Acknowledgements

Computational resources were provided by CSC — IT Centre for Science Ltd, Finland.

References

[1] Karri Muinonen, Johannes Markkanen, Timo Väisänen, Jouni Peltoniemi, and Antti Penttilä, "Multiple scattering of light in discrete random media using incoherent interactions," Opt. Lett. 43, 683-686 (2018)

[2] Muinonen, K., Nousiainen, T., Lindqvist, H., Munoz, O., and Videen, G. (2009). Light scattering by Gaussian particles with internal inclusions and roughened surfaces using ray optics. Journal of Quantitative Spectroscopy and Radiative Transfer 110, 1628-1639.

[3] Lindqvist, H., Martikainen, J., Räbinä, J., Penttilä, A., and Muinonen, K., 2018: Ray optics with inhomogeneous waves applied to scattering by ice crystals. JQSRT, under review.

[4] Martikainen, J., Penttilä, A., Gritsevich, M., Lindqvist, H., and Muinonen, K., 2018: Spectral modeling of meteorites at UV-vis-NIR wavelengths. JQSRT 204, 144–151

EPSC Abstracts
Vol. 12, EPSC2018-1120-1, 2018
European Planetary Science Congress 2018

EPSC
European Planetary Science Congress

Asteroid taxonomy with limited spectral ranges

Antti Penttilä
Department of Physics, University of Helsinki, Finland (antti.i.penttila@helsinki.fi)

1. Introduction

Asteroid taxonomic systems are classification schemes for asteroids based on their spectrophotometric properties. For the typical UV-vis-NIR wavelengths, the photometric observations probe the surface (regolith) properties of the target. As the spectral slope and the absorption bands are resulting from the light scattering mechanisms, mainly absorption, in the regolith material, the spectra contains information on the absorption coefficient of the material. Furthermore, by comparing the spectral behavior to laboratory measurements of different materials, we can find the possible mineral composition of the target.

There are several taxonomic classification systems, often created after new asteroid spectrophotometric survey program when there is novel observational data available. Some most popular examples are the Tholen taxonomy [1] using observations from the Eight-Color Asteroid Survey (ECAS), the Bus taxonomy [2] using the Small Main-Belt Asteroid Spectroscopic Survey (SMASS), and the Bus-DeMeo taxonomy [3] combining the SMASS II data with NIR observations with the SpeX instrument at the NASA infrared telescope facility. In the future, the Gaia space telescope will produce a huge data set of asteroid spectra in UV-vis-NIR range, and will most probably also produce its own taxonomic classification.

The problem with the different taxonomic systems with new observations is that they are build on the wavelengths used in their observational data set. Tholen uses eight wavelengths between 0.31 and 1.06 μm and the albedo. Bus uses wavelengths from 0.44 to 0.92 μm and with spectral resolution much higher than in ECAS. Bus-DeMeo employ wavelengths 0.45–2.45 μm, and the Gaia data will have wavelengths 0.33–1.05 μm. Now, how to classify an object if your observed spectra is not exactly from these wavelengths?

I propose here a method that is suitable for finding the Bus-DeMeo taxonomic classification for objects with observations from a spectral range that is a subset of the nominal 0.45–2.45 μm range. The method is based on the linear discriminant analysis of the original Bus-DeMeo data set of 371 asteroids that is tuned every time for the specific wavelength range, and on the Naïve Bayesian Classifier technique.

2. Spectral classifier for Bus-DeMeo taxonomy with a limited spectral range

The purpose of the method described below is to associate the spectral observation of a given target with probabilities for Bus-DeMeo (B-DM) taxonomic classes. The condition for the observed spectra is, that it is a subset of the spectral range of the original B-DM classification, that is, 0.45–2.45 μm.

For every set of spectral data with the same wavelength range $(\lambda_{low}, \lambda_{high})$, the original B-DM data of 371 asteroids is converted on-the-fly with the linear discriminant analysis (LDA) transform using the same wavelength range for the data.

The LDA is a method closely related to the principal component analysis (PCA), but with the ability for finding a new coordinate basis so that the differences *between the known classes* are maximized, whereas in PCA the classes in the data are not known beforehand. With the centered (i.e., wavelength channel means $\boldsymbol{m}$ subtracted) data matrix $\mathbf{X}$, its covariance matrix $\mathbf{S}$, and group-wise covariance matrices $\mathbf{S}_c$, the LDA is formed using the within-group and between-groups covariance matrices $\mathbf{W}$ and B as

$$\mathbf{W} = \sum_c (n_c - 1)\mathbf{S}_c,$$
$$\mathbf{B} = \sum_c n_c (\boldsymbol{m}_c^T \boldsymbol{m}_c), \quad (1)$$

where c iterates over the groups, $\boldsymbol{m}_c$ is the channel mean vector for group c, and n_c is the number of targets in group c.

From these the LDA projection matrix is constructed with the help of the eigenvalue decomposition,

$$\mathbf{L}\mathbf{\Lambda}\mathbf{L}^{-1} = \mathbf{W}^{-1}\mathbf{B}, \quad (2)$$

Now the matrix $\mathbf{L}$ holds the eigenvectors that project the spectral values to LDA-space. The eigenvalue magnitudes order the projections from the most relevant to the least relevant, and only the few first dimensions are needed. Finally, the LDA-projected data (both the original B-DM targets and the observations to be classified) is received with the transformation

$$\boldsymbol{y} = (\boldsymbol{x} - \boldsymbol{m})\mathbf{L}. \quad (3)$$

The actual classifier, the naïve Bayesian classifier (NBC), is using the LDA-transformed B-DM data (here, $\mathbf{Z}$) as a learning set to classify the new observations $\boldsymbol{y}$. The NBC treats every class as a (Gaussian) probability distribution, and our training set gives the estimated parameters to these distributions. The NBC probability for an observation $\boldsymbol{y}$ to belong to class c is therefore computed as

$$p_c = a_c \, \mathrm{f}(\boldsymbol{y}; \boldsymbol{m}_c^*, \mathbf{S}_c^*), \quad (4)$$

where f is the probability density function of multivariate Gaussian distribution, and a_c is the a priori probability of class c. The NBC probability will be computed for all the classes, and the most probable class is selected.

3. Discussion

I present here a method to relate asteroid spectral observations to the Bus-DeMeo taxonomy, even if the wavelength range of the observed spectra does not meet the range of the Bus-DeMeo system. I have selected the Bus-DeMeo taxonomy here because it offers the widest wavelength range to be used. We have tested this method in a special case with the Gaia wavelengths [4], but it can be used with all Bus-DeMeo wavelength range subsets.

References

[1] Tholen, D.J., Asteroid taxonomy from cluster analysis of photometry, Ph.D. thesis, University of Arizona, 1984.

[2] Bus, S.J., Compositional structure in the asteroid belt: Results of a spectroscopic survey, Ph.D. thesis, Massachusetts Institute of Technology, 1999.

[3] DeMeo, F.E., Binzel, R.P., Slivan, S.M., and Bus, S.J., An extension of the Bus asteroid taxonomy into the near-infrared, Icarus, Vol. 202(1), pp. 160–180, 2009.

[4] Torppa, J., Granvik, M., Penttilä, A., Reitmaa, J., Tudose, V., Pelttari, L., Muinonen, K., Bakker, J., Navarro, V., and O'Mullane, W.: Added-value interfaces to asteroid photometric and spectroscopic data in the Gaia database, Advances in Space Research, In press, doi:10.1016/j.asr.2018.04.035, 2018.

EPSC Abstracts
Vol. 12, EPSC2018-1146-1, 2018
European Planetary Science Congress 2018

Interpolating light scattering properties using spiral curve on the sphere surface

Janne Siipola (1), Antti Penttilä (1), Guanglang Xu (1), and Karri Muinonen (1,2)
(1) Department of Physics, University of Helsinki, Finland; (2) Finnish Geospatial Research Institute FGI, National Land Survey of Finland, Finland

Abstract

We introduce a grid on a sphere constructed by a spiral curve. We describe the utilization of the spiral in interpolation and integration, together with cubic splines [1]. In particular, we show how the spiral is discretized on the sphere, and how the discretization is optimized. We apply the spiral interpolation and integration to specific scattering problems illustrating the power of the scheme.

1. Introduction

In Monte Carlo radiative transfer computations, the single-scattering phase function, or in a more general case, the Mueller matrix of the scatterer, is needed in the simulation. This property is needed when drawing new direction for the light ray after a scattering event. For complex particles this property needs to be computed beforehand for each particle type. Since the phase function or the Mueller matrix is a function of the scattered direction, some discretization is needed over the 4π solid angle for these directions and the associated Mueller matrices. In this work we present a scheme for discretizing the unit sphere, and to interpolate the scattering properties for directions between these discrete directions for which the scattering properties are computed and stored.

The discretization of the unit sphere for scattering computations have been studied before, for example in Okada et al. (2008) and in Penttilä et al. (2011) [2, 3]. However, these works have mainly concentrated on the numerical averaging for the random orientation properties, i.e., integration. With this study we concentrate on the interpolation of the scattering properties for an arbitrary scattering direction, using a set of discrete directions with known properties.

For the abovementioned interpolation task, we employ the spiral curve on the surface of a unit sphere. The discrete set of directions with known properties are sampled from this curve path. The discretization of the spiral curve is done so that the distances between the points on the curve is fixed.

2. Discretized spiral curve on the sphere

The spherical spiral path φ on the surface of a sphere is given below at (1),

$$\varphi(t) = (r\sin(t)\cos(kt), r\sin(t)\sin(kt), r\cos(t)) \tag{1}$$

where $t \in [0, \pi]$. The points of the discrete grid lie on the spiral path on the surface of the unit sphere (i.e., spherical spiral) [4, 5]. The spiral path is constructed with two parameters, the number of rounds around the sphere and the number of points on the path. Points are placed with constant arc length distances to each other along the spiral path.

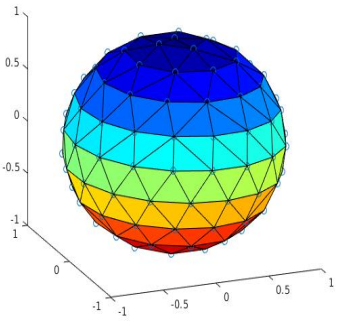

Figure 1: Spiral grid of a unit sphere

The number of points is optimized for the given number of rounds by an optimization algorithm. The discrete points can be connected into triangles by Delauny triangulation [6], and the algorithm finds the optimal number of points to so that these triangles are uniform in angles or edge lengths.

The interpolation for an arbitrary direction is carried out in the following way. At initialization, we form a cubic interpolation spline along the spherical spiral path with the abovementioned set of discrete points with known scattering properties. Then, we construct another longitudinal path from pole to pole so that it crosses the direction to be interpolated. This second path will cross the spiral path in several points, and the scattering properties can be interpolated at these crossing points with the spline on the spiral. Finally, a second cubic interpolation spline can be constructed on the longitudinal path with knots at the crossing points, with the scattering properties interpolated using the spiral spline at these knots. Using this second spline we can interpolate the properties for the given arbitrary direction.

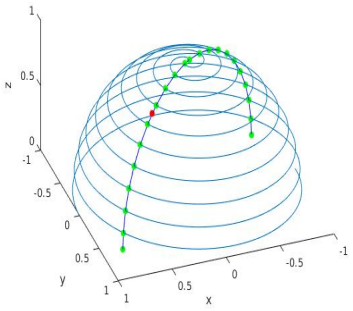

Figure 2: Paths of splines and crossing points on the hemisphere

Also integration over the unit sphere can be done with the weights to the grid points following the area of the corresponding Voronoi polygons [7, 8]. Voronoi diagram calculates fractions of the surface where the grid points are the closest inside the fraction.

Acknowledgements

The work is supported by the Academy of Finland, project 298137.

References

[1] de Boor, Carl.: A Practical Guide to Splines, Springer-Verlag, New York, 1978.

[2] Okada, Y., Mann, I., Mukai, T., and Köhler, M.: Extended calculation of polarization and intensity of fractal aggregates based on rigorous method for light scattering simulations with numerical orientation averaging, Journal of Quantitative Spectroscopy & Radiative Transfer, Vol. 109(15), pp. 2613–2627, 2008.

[3] Penttilä, A. and Lumme, K.: Optimal cubature on the sphere and other orientation averaging schemes, Journal of Quantitative Spectroscopy & Radiative Transfer, Vol. 112(11), pp. 1741–1746, 2011.

[4] Hüttig, C. and Stemmer, K.: The spiral grid: A new approach to discretize the sphere and its application to mantle convection, Geochemistry, Geophysics, Geosystems, Vol. 9(2), 2008.

[5] Chukkapalli, G., Karpik, S.R., and Ethier, C.R.: A Scheme for Generating Unstructured Grids on Spheres with Application to Parallel Computation, Journal of Computational Physics, Vol. 149, pp. 114–127, 1999.

[6] Delaunay, B.: Sur la sphère vide. A la mémoire de Georges Voronoï, Bulletin de l'Académie des Sciences de l'URSS. Classe des sciences mathématiques et na, N. 6, pp. 793–800, 1934.

[7] Aurenhamer, F.: Voronoi Diagrams — A Survey of a Fundamental Geometric Data Structure, ACM Computing Surveys, Vol. 23(3), 345–405, 1991.

[8] Voronoi, G.: Nouvelles applications des paramétres continus á la théorie des formes quadratiques. Premier mémoire. Sur quelques propriétés des formes quadratiques positives parfaites, Journal für die reine und angewandte Mathematik, Vol 1908(133), 97–102, 1908.

EPSC Abstracts
Vol. 12, EPSC2018-1259, 2018
European Planetary Science Congress 2018

Reflectance measurements of satellite materials

Antti Penttilä (1), Olli Wilkman (2), Sonja Lahtinen (2), Maria Gritsevich (1), Jesús Escobar-Cerezo (1), and Karri Muinonen (1,2)
(1) Department of Physics, University of Helsinki, Finland (antti.i.penttila@helsinki.fi); (2) Finnish Geospatial Research Institute FGI, National Land Survey of Finland.

1. Introduction

The electromagnetic radiation introduces a force, the radiation pressure, when absorbing or reflecting from a material. This force is very small and can usually be neglected on the Earth, but can be detectable for objects in space, especially when studying their orbits over time.

In our ongoing ambitious project we are relating the radiation pressure that the Global Navigation Satellite System (GNSS) satellites are experiencing to the albedo of the Earth. The albedo of the Earth is the ratio between the emitted and incident radiation by the Earth, and is a key parameter in understanding the global temperature balance of the Earth and its climate.

The main radiation component for the satellites is the direct sunlight ($\sim 10^{-6}$ pascals), but radiation reflected and emitted by the Earth is the second largest radiation component ($\sim 10^{-8}$ pascals). On the other hand, the satellite orbits are constantly observed by different satellite laser ranging stations around the globe. With the models for their orbits, one can remove all the other known effects and observe the radiation pressure force component that they are experiencing at different times and positions. This force component is now due to the radiation component from the Earth. By observing many satellites at the same time we invert the global albedo, integrated over the 4π solid angle, of the Earth.

One parameter that is needed in the model is the reflectance and absorption properties of the GNSS satellites. These quantities need to be measured for the typical satellite surface materials.

2. Optical properties of satellite materials

We will acquire typical surface materials of satellites, with the typical solar panel materials being the most important regarding the radiation pressure. We will measure the spectral bi-directional reflectance distribution function (spectral BRDF) of these with our LightTec Reflet 180S spectro-goniometer. This device can measure the angular reflectance with any illumination direction. This can be done with visual- and near-infrared wavelengths up to 1 µm.

For ultraviolet (starting from 0.25 µm) and near-infrared up to 3.2 µm, we can measure the integrated (over the hemisphere) reflectance spectra with our Gooch & Housego OL750 spectroradiometric system [1]. The spectral BRDF for these wavelengths can be estimated by combining the BRDF for other wavelengths with the albedo integrated over the hemisphere for these wavelengths.

The measured spectra are finally applied to 3D satellite shape models in a simulation of spacecraft reflection properties. This simulation can be used to model e.g. photometry, spectrometry and radiation pressure forces on satellites.

Acknowledgments

The work is supported by the Academy of Finland, project 298137.

References

[1] Penttilä, A., Martikainen, J., Gritsevich, M., and Muinonen, K.: Laboratory spectroscopy of meteorite samples at UV-vis-NIR wavelengths: Analysis and discrimination by principal components analysis, Journal of Quantitative Spectroscopy & Radiative Transfer, Vol. 206, pp. 189–197, 2018.

EPSC Abstracts
Vol. 12, EPSC2018-1269, 2018
European Planetary Science Congress 2018

Validation of light scattering models with advanced 4π scatterometry

M. Gritsevich (1), A. Penttilä (1), G. Maconi (1), P. Helander (1), I. Kassamakov (1), J. Martikainen (1), J. Markkanen (2), T. Väisänen (1), J. Blum (3), T. Puranen (1), A. Salmi (1), E. Hæggström (1), and K. Muinonen (1,4)
(1) Department of Physics, University of Helsinki, Gustaf Hällströmin katu 2a, Helsinki, Finland (maria.gritsevich@helsinki.fi), (2) Max Planck Institute for Solar System Research, Göttingen, Germany, (3) Institut für Geophysik und Extrater-restrische Physik, Technische Universität Braunschweig, Germany, (4) Finnish Geospatial Research Institute (FGI), Masala, Finland.

Abstract

Within the ERC Advanced project 'SAEMPL' we have developed a novel orientation-controlled scatterometer – an instrument for precise full Mueller matrix measurement of light scattered by a mm- to µm-sized sample manipulated by ultrasound. The orientation of the sample is controlled by the custom-built acoustic levitator to allow non-destructive light scattering measurement in any solid angle, providing a full 4π measurement result. Additionally, high speed camera monitoring the sample is used for a photogrammetric 3D shape reconstruction of the sample. By providing robust experimental data for well-characterized samples we enable verification of the state-of-the-art light scattering models. Moreover, non-destructive non-contact measurements are also important for characterizing unique and valuable samples, such as cosmic dust and planetary samples.

1. Introduction

Computational Electromagnetics methods are used for modeling the light scattering response of single particle to more elaborate targets. These methods are computationally expensive and limited with respect to the size of the scatterer, compared to the wavelength [1]. On the other hand, scattering experiments, along with the sample characterization, are more convenient when done with particles moving in a flow, particle agglomerates, or particulate surfaces [2-5]. The aim of our project was to bridge this gap by going beyond the state of the art in both, theory and experiment.

One of the first scatterometry setups for small particle characterization was built in Arizona [6]. The system was used to characterize 110 nm diameter latex spheres. A more recent system was built in Amsterdam [7], and further developed at the IAA cosmic dust laboratory in Granada [2], to measure scattering properties of irregularly shaped mineral samples. The main difference between these systems and our instrument is that they measure the statistical average of a flow of 'running' particles. On the other hand, the levitator keeps sample still, while absence of interfering sample holder in our experimental setup allows non-destructive non-contact measurements of well-characterized sample in all orientations [8].

2. Theoretical pipeline

For theoretical computations we utilize SAEMPL software suite, where light-scattering characteristics of the sample are modeled using novel multiple scattering methods for close-packed random media, such as a geometric optics method SIRIS4 [9] and the radiative transfer with reciprocal transactions R^2T^2 [10]. The R^2T^2 method solves the ensemble-averaged Foldy-Lax equation involving the ladder and maximally crossed diagrams as well as the near field corrections. The near field corrections are implemented in terms of the incoherent volume element containing all the scattering diagrams that do not cancel out in the near-zone [10]. The incoherent scattering parameters of the volume elements are solved exactly by the fast superposition T-matrix method [11]. The latter enables us to extend the applicability of the radiative transfer to close-packed random media [10].

3. Design of the scatterometer

The developed scatterometer comprises 4 parts, based on their function: the light source, the sample levitator, the analyzer, and the monitoring camera:

• The light source is a laser-stabilized arc lamp producing white light, which is then filtered by a line filter and polarized by a linear polarizer. A reference photomultiplier tube (PMT) is used for monitoring the

beam intensity, and the signal can be used to calibrate the observed signal power level.

• The acoustic levitator is custom built and features 400 transducer elements, grouped into 28 phase controlled channels. The resulting two hemispherical phased arrays produce an asymmetric acoustic trap which holds the sample in place at an adjustable orientation (heading, pitch and roll).

• The analyzer comprises a PMT with an integrated solid state high speed shutter, a motorized quarter wave plate, a motorized linear polarizer, and a motorized shutter. It is mounted on a large, motorized rotation stage, allowing it to scan the scattered light with an angular accuracy of 15'.

• The camera monitoring system allows to verify the stability of the ultrasonic levitation and orientation control. It features a high speed camera and near infrared LED illumination.

4. Validation results

With cross-validation purposes application of the software suite to the defined close-packed random media is followed by comparison with the experimental results. Among suitable planetary analogue samples for the experimental study we have defined, among others, macroscopic agglomerates formed by ballistic hit-and-stick deposition. The agglomerates consist of monodisperse SiO_2 spheres of known radius. The light-scattering characteristics of the formed of SiO_2 spheres agglomerates are thoroughly measured with the scatterometer. The shape and the packing density of the agglomerates are then obtained to independently enter into the theoretical pipeline along with the used in the measurements incident light wavelength and the refractive index of the sample material. The results obtained by studying the agglomerates composed of monodisperse SiO_2 spheres demonstrate, that application of the software suite for analyzing optical properties of close-packed random media matches well with the experimental results obtained using the described orientation-controlled scatterometer.

Acknowledgments

The ERC Advanced Grant No. 320773.

References

[1] Mishchenko, M.I., Travis, L.D., Lacis, A.A., Scattering, absorption and emission of light by small particles. Cambridge University Press (2002).

[2] Muñoz, O., Moreno, F., Guirado, D., Ramos, J. L., López, A., Girela, F., Jerónimo, J. M., Costillo, L. P., Bustamante, I., Experimental determination of scattering matrices of dust particles at visible wavelengths: The IAA light scattering apparatus. JQSRT 111(1), 187-196 (2010).

[3] Videen, G., Kocifaj, M. (Eds.), Optics of cosmic dust (NATO Science Series). Kluwer Academic Publishers (2002).

[4] Peltoniemi, J. I., Gritsevich, M., Hakala, T., Dagsson-Waldhauserová, P., Arnalds, Ó., Anttila, K., Hannula, H.-R., Kivekäs, N., Lihavainen, H., Meinander, O., Svensson, J., Virkkula, A., de Leeuw, G. Soot on snow experiment: bidirectional reflectance factor measurements of contaminated snow. The Cryosphere 9, 2323–2337, 2015.

[5] Zubko N., Gritsevich M., Zubko E., Hakala T., Peltoniemi J.I., Optical measurements of chemically heterogeneous particulate surfaces. JQSRT 178, 422-431 (2016).

[6] Hunt, A. J., Huffman, D. R., A new polarization-modulated light scattering instrument. Review of Scientific Instruments, 44(12), 1753-1762 (1973).

[7] Volten, H, Munoz, O, Rol, E, de Haan, JF, Vassen, W, Hovenier, JW, Muinonen, K, Nousiainen, T. Scattering matrices of mineral aerosol particles at 441.6 nm and 632.8 nm. Journal of Geophysical Research: Atmospheres, 106, 17375-17401, 2001.

[8] Maconi G., Penttilä A., Kassamakov I., Gritsevich M., Helander P., Puranen T., Salmi A., Hæggström E., Muinonen K. (2018): Non-destructive controlled single-particle light scattering measurement. JQSRT, 204, 159–164.

[9] Martikainen J., Penttilä A., Gritsevich M., Lindqvist H., Muinonen K. (2018): Spectral modeling of meteorites at UV-vis-NIR wavelengths. JQSRT, 204, 144–151.

[10] Muinonen K., Markkanen J., Väisänen T., Peltoniemi J., Penttilä A. (2018) Multiple scattering of light in discrete random media using incoherent interactions. Optics Letters 43(4):683–686.

[11] Markkanen J. and Yuffa A. J. (2017) Fast superposition T-matrix solution for clusters with arbitrarily-shaped constituent particles. JQSRT 189:181–189.